ARTICLE

BIOTECHNOLOGY BIOENGINEERING WILEY

Activity of a hypochlorous acid-producing electrochemical bandage as assessed with a porcine explant biofilm model

Gretchen Tibbits[1] | Abdelrhman Mohamed[1] | Suzanne Gelston[1] |
Laure Flurin[2] | Yash S. Raval[2] | Kerryl E. Greenwood-Quaintance[2] |
Robin Patel[2,3] | Haluk Beyenal[1]

[1]The Gene and Linda Voiland School of Chemical Engineering and Bioengineering, Washington State University, Pullman, Washington, USA

[2]Divison of Clinical Microbiology, Mayo Clinic, Rochester, Minnesota, USA

[3]Division of Public Health, Infectious Diseases and Occupational Medicine, Mayo Clinic, Rochester, Minnesota, USA

Correspondence
Haluk Beyenal, School of Chemical Engineering and Bioengineering, Voiland College of Engineering and Architecture, Washington State University, Pullman, WA, USA.
Email: beyenal@wsu.edu

Abstract

The activity of a hypochlorous acid-producing electrochemical bandage (e-bandage) in preventing methicillin-resistant *Staphylococcus aureus* infection (MRSA) infection and removing biofilms formed by MRSA was assessed using a porcine explant biofilm model. e-Bandages inhibited *S. aureus* infection ($p = 0.029$) after 12 h (h) of exposure and reduced 3-day biofilm viable cell counts after 6, 12, and 24 h exposures ($p = 0.029$). Needle-type microelectrodes were used to assess HOCl concentrations in explant tissue as a result of e-bandage treatment; toxicity associated with e-bandage treatment was evaluated. HOCl concentrations in infected and uninfected explant tissue varied between 30 and 80 μM, decreasing with increasing distance from the e-bandage. Eukaryotic cell viability was reduced by an average of 71% and 65% in fresh and day 3-old explants, respectively, when compared to explants exposed to nonpolarized e-bandages. HOCl e-bandages are a promising technology that can be further developed as an antibiotic-free treatment for wound biofilm infections.

KEYWORDS
biofilms, chronic wounds, electrochemical bandage, hypochlorous acid, MRSA, *Staphylococcus aureus*

1 | INTRODUCTION

An estimated 2% of the United States population struggles with chronic wounds, a significant burden for affected patients and an over $50 billion per year cost to the healthcare system (Driver et al., 2010; Sen et al., 2009). The presence of pathogenic biofilms in the wound-beds hinders the normal process of wound recovery (Metcalf & Bowler, 2013; Rhoads et al., 2012; Sen, 2019). Biofilms are aggregates of microorganisms that express extracellular polymeric substance (EPS) which acts as a protective barrier against

hazards to the cells within (Davenport et al., 2014; Lewandowski & Beyenal, 2013). Biofilms are associated with chronic wounds, such as nonhealing surgical and traumatic wounds, diabetic foot ulcers, venous leg ulcers, and pressure ulcers (Dowd et al., 2008). Microorganisms within biofilms alter the wound bed environment by secreting toxins and/or enzymes, creating alkaline conditions, or reducing oxygen concentration in the wound bed (Chaney et al., 2017; Lone et al., 2015; Nakatsuji et al., 2016). Biofilms also tolerate several fold-increased concentrations of antibiotics compared to planktonic bacteria (Nadell et al., 2009; Uruén et al., 2021). Chronic biofilms

causing wound infections pose a significant challenge to human health; therefore, development of technologies to remove existing biofilms or prevent biofilm formation is desirable.

Staphylococcus aureus is a common pathogen in wound biofilms. Particularly, methicillin-resistant *S. aureus* (MRSA) is concerning as it is more challenging to treat than is its methicillin-susceptible counterpart (Hiramatsu et al., 1997; Koch et al., 2014; Walsh & Wencewicz, 2016). *S. aureus* utilizes multiple mechanisms to survive antibiotics and the immune system response by invading phagocytes such neutrophils (Bien et al., 2011) or by burrowing into the dermis (Chaney et al., 2017; Sayedyahossein et al., 2015). *S. aureus* infections in patients who have reduced immune and inflammatory responses due to factors such as chemotherapy, diabetes, or cystic fibrosis may be even more challenging to treat (Gupta et al., 2016; Høiby et al., 2011).

Hypochlorous acid (HOCl), a common biocide, is active against MRSA (Raval et al., 2021; Ulfig & Leichert, 2021). Theoretically, wound dressings that deliver sustained low HOCl concentrations could be developed as an antibiotic-free treatment approach to manage MRSA biofilm infections. However, there has not been a good system available to deliver HOCl continuously. Accordingly, we developed HOCl-generating electrochemical scaffolds which produce controlled low concentrations of HOCl and demonstrated their activity in in vitro biofilm models (Flurin et al., 2021; Kiamco et al., 2019; Raval et al., 2021; Zmuda et al., 2020); however, those devices needed to be submerged in liquid to work, an untenable configuration for treating wound biofilms. To overcome this limitation, we recently described an electrochemical bandage (e-bandage) that allows sustained delivery of electrochemically-generated HOCl (Mohamed et al., 2021). e-Bandages use a xanthan-gum-based hydrogel to provide electrolytic conductivity between the electrodes, rather than requiring submersion in liquid. HOCl is generated electrochemically by oxidizing chloride ions (Cl$^-$) to chlorine gas (Cl$_2$) following the reaction: $2Cl^- \rightleftharpoons Cl_2 + 2e^-$ E$_o$ = +1.138V$_{Ag/AgCl}$ (Rumble, 1978). Chloride ions are prevalent in wound environments and are added to the hydrogel at physiological concentrations to provide an isotonic environment. Cl$_2$ gas dissociates in water to produce HOCl following the reaction: $Cl_2 + H_2O \rightleftharpoons Cl^-_{(aq)} + HOCl_{(aq)} + H^+_{(aq)}$. As demonstrated in the literature, electrochemical methods can be utilized to control and/or monitor the interfacial microenvironment where inert metal electrodes interact with biological systems (Ehrensberger et al., 2020; Sultana et al., 2015). Huiszoon et al. (2021) built a system comprised of flexible, interdigitated electrodes incorporated into a urinary catheter via a 3D-printed insert for impedance sensing and bioelectric effect-based treatment (Huiszoon et al., 2021). Heald et al. (2022) treated infected chronic wounds in a dog and a cat using electroceutical dressings by applying up 0.6 mA direct current (Heald et al., 2022).

The use of porcine explants has been reported to simulate wound infections (Jensen et al., 2017; Sullivan et al., 2001), to assess anti-infection or -biofilm activities of new devices (McMahon et al., 2020; Phillips et al., 2015; Yang et al., 2013; Yang et al., 2017), to study the efficacy of wound cleansers and antimicrobial agents against infections (Alves et al., 2018; McMahon et al., 2020; Roberts et al., 2019; Roche et al., 2019; Y. Wang et al., 2018; H. Wang et al., 2021), and to assess the toxicity to tissue due to HOCl (Zmuda et al., 2020).

The goal of this study was to evaluate the HOCl-producing e-bandages against MRSA biofilms grown on porcine explants, and assess potential toxicity to porcine tissue. The efficacy of HOCl generating e-bandages was assessed by quantifying biofilm cell counts under two conditions: (1) infection prevention, and (2) biofilm removal. Potential toxicity was assessed using uninfected explants. HOCl concentration-depth profiles were measured using needle-type microelectrodes to monitor HOCl penetration into biofilms and explant tissue.

2 | METHODS AND MATERIALS

2.1 | HOCl-producing e-bandage

HOCl-producing e-bandages were constructed as previously described (Mohamed et al., 2021), and autoclaved for 15 min at 121°C before use against biofilms. e-Bandages were polarized at 1.5V$_{Ag/AgCl}$ to generate HOCl. e-Bandages are a three-electrode system consisting of a conductive carbon fabric (Panex 30 PW-06, Zoltek) as working and counter electrode, and an Ag/AgCl reference wire as a reference electrode. e-Bandages were applied with the working electrode facing the biofilm. A Gamry Interface1000 potentiostat and Gamry ECM8 were used to control working electrode potential (Gamry Instruments).

### 2.2 | Chemicals, supplies, and bacteria

Dulbecco's Modified Eagle Medium (DMEM) without dilution (Thermo Fisher Scientific, # 21063029) and 100× antibiotic-antimycotic (initial concentration: 10,000 units/ml penicillin, 10,000 µg/ml streptomycin, and 25 µg/ml amphotericin B, Thermo Fisher, cat no. 15240096) were used as purchased. Phosphate saline buffer solution (PBS) contained 0.01 mol/L Na$_2$HPO$_4$, 1.8 mmol/L KH$_2$PO$_4$, 0.137 mol/L NaCl, and 2.7 mmol/L KCl. Hydrogel was prepared by dissolving 1.8 wt% xanthan gum (Namaste Foods LLC, Coeur d'Alene, ID) into 500 mL of PBS. Tryptic soy broth (TSB, BD™ cat no. 211825) and tryptic soy agar (TSA, BD™ cat no. 236950) were prepared at full strength and autoclaved for 15 min at 121°C. 1.8 wt% TSA was used for colony forming unit (CFU) quantification before and after treatment. TSA plates with 1× antibiotic-antimycotic concentration (10 units/ml penicillin, 10 µg/ml streptomycin, and 0.025 µg/ml amphotericin B) were used for uninfected explants (cell viability) and called 1× antimicrobial agent TSA plates. TSA plates with 0.1× antibiotic/antifungal concentration (1 unit/ml penicillin, 1 µg/ml streptomycin, and 0.0025 µg/ml amphotericin B) were used for infected explants (infection prevention and biofilm removal) and are hereafter referred to as 0.1× antimicrobial agent TSA plates. A clinical isolate of MRSA (IDRL-6169) was studied.
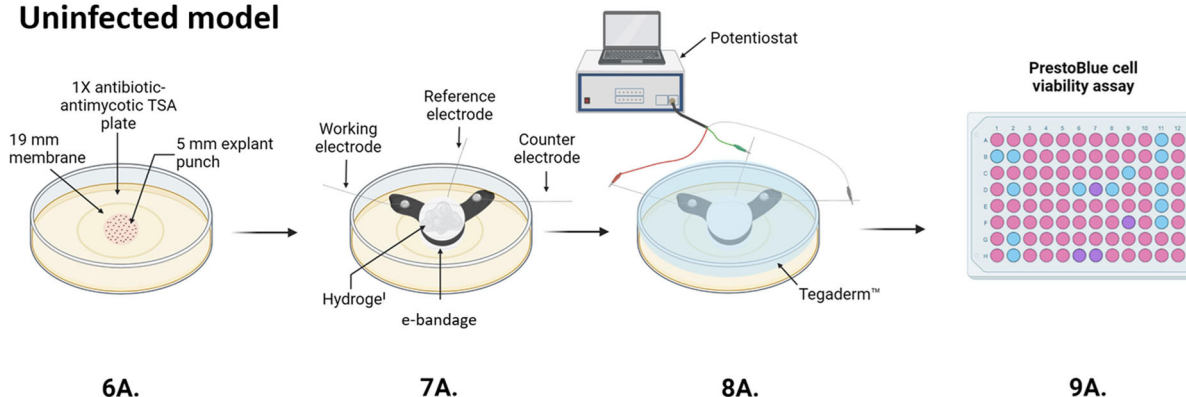
2.3 | Porcine explant preparation

Porcine explant preparation was adapted from our prior work (Zmuda et al., 2020) to accommodate an agar model. Briefly, explants were harvested from fresh pig ears (same day) from local meat processing facilities, cooled to 4°C and transported to the laboratory for processing. Initial processing included scrubbing with 10% all-purpose cleaner (Walmart, cat no. 22301219) under cold water, hair removal using an electric razor, and scrubbing with 10% povidone-iodine solution (Walmart, cat no. 236247392) and gauze sponges for 10 min followed by 5 min inside of a biological safety cabinet (Figure 1.1). The outer rim of the ear was then removed using a single-use sterile razor blade and cut into 3 to 4 pieces (Figure 1.2). The epidermis was removed using a Padgett's dermatome (Nouvag TCM 3000) set to 500-μm and discarded (Figure 1.3); then, a 500-μm layer of the dermis was removed using the dermatome (Figure 1.4). The 500-μm dermis tissue was then sectioned into 5-mm discs with a biopsy punch (Robbins Instruments Part No. RBP-50) (Figure 1.5) and placed on UV-sterilized 19-mm 0.2-μm polycarbonate membranes (Cytivia Life Sciences, cat no. 10417001) on 1× antimicrobial agent TSA plates (cell viability) or 0.1× antimicrobial agent TSA plates (infection models). Uninfected and infected explants were stored in an incubator with 5% CO_2 and 95% humidity at 37°C.
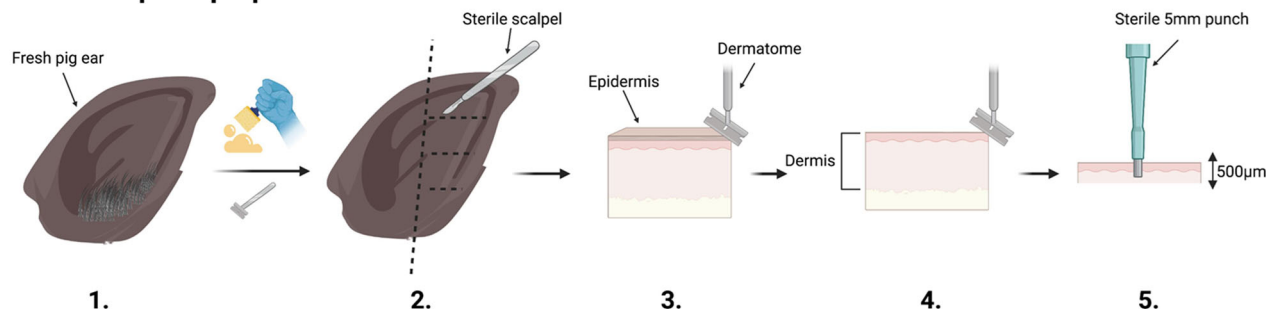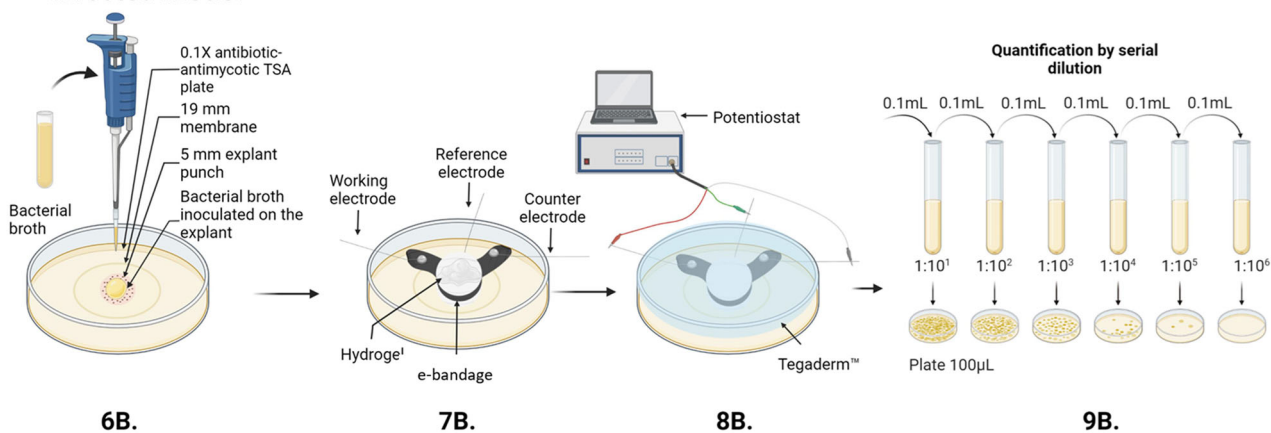

FIGURE 1 Schematic of porcine explant preparation (1–5), uninfected model (6A–9A), infected model experiments (6B–9B), e-bandage placement and connection to potentiostat (7–8), PrestoBlue cell viability assay (9A), serial dilution and CFU quantification (9B). The figure was prepared using BioRender©, and modified from (Tibbits et al., 2022).

The detailed protocol can be found in Supplementary Information (Detailed Explant Preparation Protocol).

2.4 | Viability of eukaryotic cells

Uninfected explants were used to assess potential toxicity due to HOCl e-bandage treatment. For explants exposed to e-bandages on Day 0, e-bandage exposure started immediately after processing. 3-day explants were placed on 1× antimicrobial agent TSA plates and transferred to fresh 1× antimicrobial agent TSA plates every 24 h while being maintained in a 5% CO_2 and 95% humidity incubator at 37°C (Figure 1.6a). Before e-bandage exposure, a total volume of 300 μl of hydrogel was dispensed: 100 μl on the explant, 100 μl inside of the PBS-soaked e-bandage, and 100 μl on top of the e-bandage (Figure 1.7a). The PBS-soaked e-bandage was placed with the working electrode facing the explant. Tegaderm™ (3 M, cat no. 16002) was used to secure the position of the e-bandage on top of the explant (Figure 1.8a). Following e-bandage exposure, explants were transferred to 96-well plates with 180 μl of DMEM and 20 μl of PrestoBlue cell viability (ThermoFisher, cat. no. A13261, Figure 1.9a). Explants were incubated for 3 h in an incubator with 5% CO_2 and 95% humidity at 37°C. Fluorescence was measured by excitation at 535 nm and emission at 590 nm using a Cytiation5 image reader (Biotek, Figure 1.9a). Normalized cell viability and reduced cell viability by polarized e-bandages were calculated using equations found in the Supplementary Information (equations for calculation of normalized cell viability).

2.5 | S. aureus infection model

Two infection conditions were tested: infection prevention and biofilm removal. Frozen stock culture was used to prepare generation 1 and generation 2 streak plates on blood agar (grown overnight for 24 h) (Trypticase™ Soy Agar II with 5% sheep blood, BD™ Cat. No. 254087). A single colony from the generation 2 streak plate was suspended in 5 mL of TSA and incubated for 2 to 2.5 h at 37°C to achieve 7.8 ± 0.2 $\log_{10}$ CFU/cm^2 (0.5 McFarland). For the infection prevention model, 10 μl of 0.5 McFarland S. aureus was inoculated onto fresh explants, immediately followed by e-bandage exposure (Figure 1.6b). Infection prevention experiments were conducted at 37°C. For biofilm removal, explants were inoculated with 2.5 μl of 0.5 McFarland S. aureus and biofilms allowed to grow for 3 days. Infected explants were transferred to fresh 0.1× antimicrobial agent TSA plates every 24 h, and kept in an incubator at 5% CO_2 and 95% humidity at 37°C. e-Bandage exposure was conducted at room temperature. e-Bandage placement and setup were identical to eukaryotic cell viability experiments (Figure 1.7–9b). After e-bandage exposure, e-bandages were rinsed with 5 mL of PBS. The PBS was combined with the explant and membrane and vortexed for 30 s, then sonicated in a water bath for 5 min and vortexed again for 30 s. Finally, the solution was centrifuged for 10 min at 5000 rpm (2910 × g), supernatant removed, and the bacterial pellet resuspended in 1 ml of fresh PBS. The resuspension was serial diluted 10-fold in

PBS and spread onto TSA plates for CFU quantification 24 h later (Figure 1.9b).

2.6 | Hypochlorous acid concentration profiles in porcine explants

Needle-type HOCl microelectrodes were constructed similarly to previous work and used an external leakless Ag/AgCl reference electrode (similar to EDAQ ET072-1) (Lewandowski & Beyenal, 2013). Briefly, microelectrodes were constructed by tapering a 50 μm platinum wire to a several micrometer tip (California Fine Wire Company Pure TC Grade) sealed into a glass capillary (Corning 8161). Platinum was electrodeposited on the microelectrode tip to create a 20 – 30-diameter μm ball. The microelectrode tip was dipped into a 5% cellulose acetate solution and dried for 24 h. The microelectrode was calibrated before and after each concentration profile with a NaOCl standard solution in PBS (pH = 7.4) and polarized at $0.8V_{Ag/AgCl}$ relative to an external leakless Ag/AgCl reference electrode using a G300 Gamry Potentiostat (Gamry Instruments). The microelectrodes had a sensitivity of 50–100 nA/μmol·L and a 10 μM limit of detection.

Microelectrode measurements were performed immediately after removing the e-bandage from 12 h non-polarized or polarized e-bandage explants (infected and uninfected). The microelectrode tip was controlled using a custom LABVIEW script and positioned at the surface of the explant using a Zeiss Stermi 2000 stereomicroscope – determined visually (Carl Ziess Microscopy). The microelectrode tip was then retracted by 3 mm from the surface, and 100 μl of hydrogel was added on top of the explant. The concentration-depth profile was measured at 25 μm intervals from 200 μm above the surface to 300 μm into the explant. Microelectrodes were polarized for 3 min before the measurement to limit the contribution of transient current response.

2.7 | Scanning electron microscope imaging of porcine explants

Immediately following HOCl e-bandage exposure, explants were placed in a solution of 2% paraformaldehyde/2% glutaraldhyde and stored at 4°C. Explants were then washed with 0.1 M phosphate buffer twice for 15 min to rinse the fixative solution. Explants were dehydrated by single 15 min ethanol treatments at 10%, 30%, 50%, 70%, and 90% followed by two 15 min treatments in 100% ethanol and critical point dried (Samdri-PVT 3B). Finally, explants were placed onto stubs and gold sputter coated (Sputter Coater Technics Hummer V – Gold) and imaged using an SEM FEI Apreo microscope.

2.8 | Statistical analysis

A two-sided Wilcoxon rank-sum test was used to assess the statistical significance between treatments. $p < 0.1$ was considered

statistically significant. Experiments were performed in quadruplicate, except when supply limitations of pig ears meant experiments could only be replicated three times. Standard deviations, means, and individual data points are presented in the figures. Replicate experiments were performed on different days.

3 | RESULTS AND DISCUSSION

3.1 | e-bandages prevent *S. aureus* biofilm formation and remove mature biofilms from explants

e-Bandages prevented growth of *S. aureus* biofilms on porcine explants. No e-bandage and non-polarized e-bandage-exposed explant biofilms grew to 5.2 ± 1.1 and 6.6 ± 0.9 $\log_{10}$ CFU/cm^2,
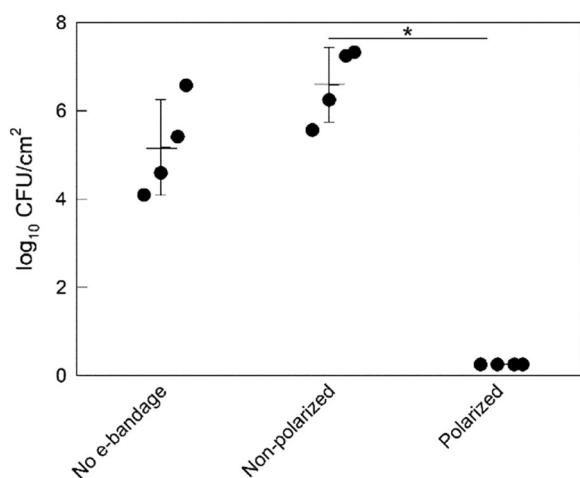

FIGURE 2 Evaluation of HOCl e-bandages for porcine explant *Staphylococcus aureus* infection prevention. Polarization started immediately following explant inoculation with *S. aureus*. Data points representing individual replicates are shown using circles. Horizontal lines and error bars represent averages and standard deviations. Statistical significance is indicated by a star ($n = 4$).

respectively (Figure 2) whereas viable cell counts after 12 h of e-bandage treatment were below the limit of detection [0.25 $\log_{10}$ CFU/cm^2 ($p = 0.029$)]. This demonstrates the e-bandages prevent *S. aureus* biofilm formation on porcine explants.

e-Bandage treatment showed a time-dependent response against mature (3-day-old) *S. aureus* biofilms on porcine explants. After 3 days of growth, *S. aureus* biofilms had an average biofilm density of 9.3 ± 0.45 $\log_{10}$ CFU/cm^2. Viable cells in *S. aureus* biofilms did not change in control (no e-bandage) or nonpolarized e-bandage treatment groups over 6, 12, and 24 h ($p > 0.1$) (Figure 3). 3-day *S. aureus* biofilms treated with polarized e-bandages for 6, 12, and 24 h. were reduced to 7.45 ± 1.03 $\log_{10}$ CFU/cm^2 (reduction of 1.74 ± 1.17 $\log_{10}$ CFU/cm^2 [$p = 0.029$], Figure 3a), 5.66 ± 0.96 $\log_{10}$ CFU/cm^2 (reduction of 4.11 ± 0.92 $\log_{10}$ CFU/cm^2 [$p = 0.029$], Figure 3b), and 2.9 ± 0.67 $\log_{10}$ CFU/cm^2 (reduction of 6.56 ± 0.70 $\log_{10}$ CFU/cm^2 [$p = 0.057$], Figure 3c), respectively. Reduction in biofilm was correlated with the polarized treatment time ($R^2 = 0.98$) (Figure S1). Collectively, the data demonstrate e-bandage treatment to be effective against mature *S. aureus* biofilms in a porcine explant biofilm model.

HOCl is produced as a part of the natural immune system response, contributes to the killing of phagocytized pathogens and is generated by the catalyzed reaction of myeloperoxidase with H_2O_2 (Ulfig & Leichert, 2021). HOCl kills bacteria by penetrating the cell wall and inhibiting DNA synthesis, protein synthesis, growth, and ATP production (Kiamco et al., 2019; Winter et al., 2008). HOCl producing e-bandages could be used to mimic and augment the natural immune response. In the porcine explant biofilm model, e-bandages were effective in preventing biofilm formation, and in the treatment of mature biofilm infections.

3.2 | Scanning electron microscopy (SEM) imaging of infected and uninfected explants

SEM images of uninfected and infected explants with no e-bandages, nonpolarized e-bandages, or polarized e-bandages are shown in the

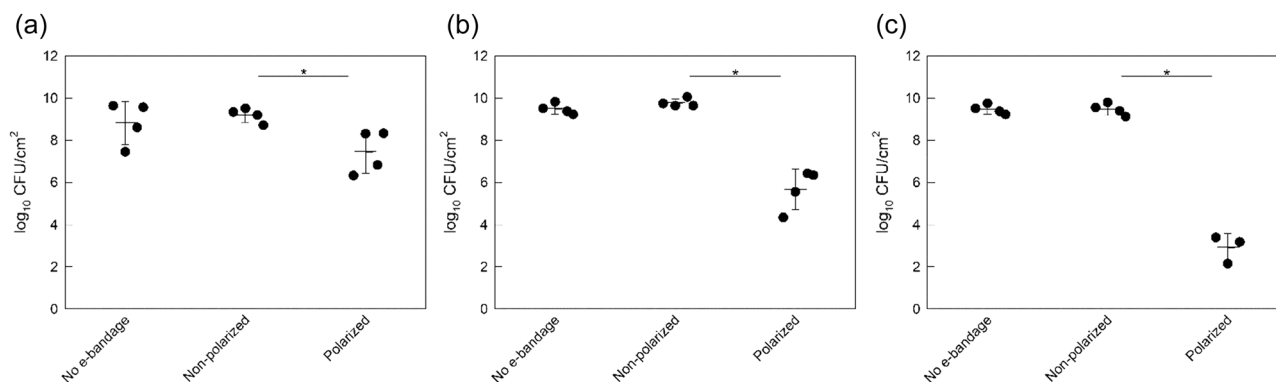**FIGURE 3** Colony forming units of *Staphylococcus aureus* biofilms grown on porcine explants for 3 days after (a) 6 h (h), (b) 12 h, and (c) 24 h exposure to no e-bandages, nonpolarized e-bandages, or polarized e-bandages. Data points representing individual replicates are shown using circles. Horizontal lines and error bars represent averages and standard deviations. Statistical significance is indicated with a star ($n \geq 3$).

Supplementary Information. Non-e-bandage-exposed uninfected (Figures S2A, S4A, S6A, and S8A) and infected (Figures S1A, S3A, S5A, and S7A) explants showed well-defined surface dermal fibers. Spherical-shaped *S. aureus* cells were observed on the surface of the infected explants and between the fibers. Nonpolarized explant-exposed dermal fibers of both infected (Figures S1B, S3B, S5B, and S7B) and uninfected (Figures S2B, S4B, S6B, and S8B) explants remained well-defined and no morphological changes in *S. aureus* cells were observed. Polarized e-bandage exposed infected (Figures S1C, S3C, S5C, and S7C) and uninfected (Figures S2C, S4C, S6C, and S8C) explant tissue showed morphological changes; some fibers appeared to be damaged, and a crust was observed on the surface. No morphological changes in *S. aureus* cells were observed after polarized e-bandage treatment. Higher surface coverage of *S. aureus* cells on the explants was observed on the 3-day explants compared to the 12 h explants (at the end of the infection prevention model), corroborating the *S. aureus* cell quantification data (Figures 2 and 3). Yang et al. observed minimal surface damage of explants when treated with 0.6% sodium hypochlorite for 30 or 60 min (Yang et al., 2013), but these treatments were significantly shorter than the e-bandage treatments described herein. On the other hand, Lochab et al. (2020) imaged *Pseudomonas aeruginosa* lawn biofilms under in vitro electroceutical treatment using a two-electrode system and found (1) significant bacterial cell damage over the anode after 24 h of treatment; and (2) a mix of both damaged and undamaged cells over the cathode. It is difficult to compare our images with theirs since (1) in our system, cells were grown on explant surfaces; and (2) we controlled potential to assure HOCl generation. In their system, a 6 V battery pack with a ballast resistor was used, and the current was approximately 3.5 mA initially and reduced to approximately 100 μA at 24 h. Since both electrochemical and biological systems were different, it is not meaningful to compare the differences in cell morphology.

3.3 | HOCl concentration profiles

Depth profiles of HOCl concentrations are shown in Figure 4. The concentration of HOCl measured in explants immediately after processing or after exposure to non-polarized e-bandages (infected and uninfected) was below the limit of detection of the micro-electrode (<10 μmol/L). HOCl was only detected in the hydrogel and explant with polarized e-bandage exposure. HOCl concentrations were between 40 and 50 μmol/L in the hydrogel above uninfected explants and 50–80 μmol/L in infected explants. HOCl was also detected as far as 300 μm below the surface of the explant in both infected and uninfected explants. Measurements were conducted for 2 biological replicates on different infected/uninfected explants under polarized and non-polarized conditions. Because of limited numbers of explants and difficulty associated with the measurements, measurements were limited to two biological replicates.

Decreased concentrations of HOCl at increasing distances from explant surfaces may be a result of consumption during *S. aureus* killing or nonspecific reactions with tissue components, such as proteins (Hawkins, 2019). The concentration of HOCl between infected and uninfected explants also varied. The HOCl concentration-depth profiles demonstrate that HOCl was generated using polarized e-bandages and transported to biofilms and explant tissue. Since non-polarized e-bandages did not show biocidal activity, the anti-biofilm activity of polarized e-bandages was mostly due to electrochemically-generated substances, including HOCl (Figures 2 and 3). Previous reports document that *S. aureus* is able to survive antibiotics and the immune system (Bien et al., 2011) by burrowing into the dermis (Chaney et al., 2017; Sayedyahossein et al., 2015). HOCl-generating e-bandages could be effective against *S. aureus* infections due to transport of electrochemically-generated HOCl into biofilms and tissue.
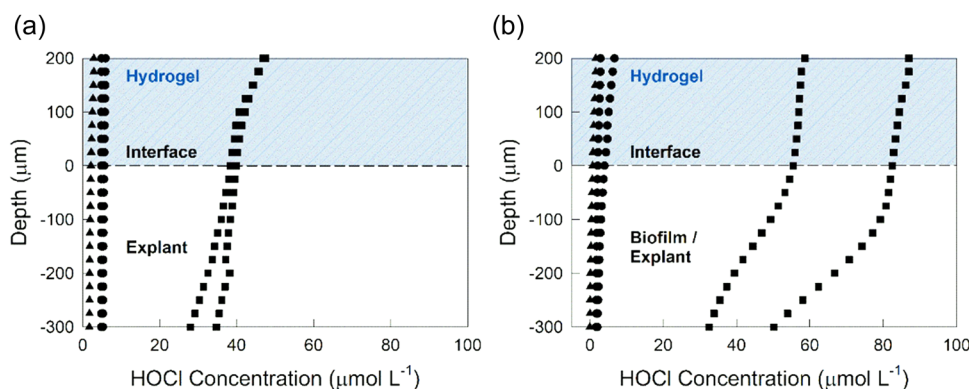

FIGURE 4 HOCl concentration-depth profiles in explant tissue and overlying hydrogel layer: (a) uninfected and (b) infected explants. HOCl was only detected when e-bandages were polarized. ▲ control explants with no e-bandages; ● explant after exposure to non-polarized e-bandages for 12 h; and ■ explant exposed to polarized e-bandages for 12 h.

3.4 | Eukaryotic cell viability

Eukaryotic cell viabilities for non-polarized e-bandage- and no e-bandage-exposed explants were similar (*p* > 0.1) (Figures 5 and 6), demonstrating no toxicity from the e-bandage material itself. Polarized e-bandages placed on explants immediately after processing resulted in 71 ± 10% reduction in viability when compared to non-polarized e-bandages (Figure 5, *p* = 0.029). Viability of 3-day-old explants exposed to polarized e-bandages was reduced by 73 ± 17%, 63 ± 12%, and 59 ± 6.5% after 6, 12, and 24 h exposures, respectively (Figure 6, *p* = 0.029). Reduction in viability was independent of treatment starting time or treatment time (*p* > 0.1).

Explant tissue viability was maintained by diffusion of nutrients and moisture from nutrient agar. As such, tissues had limited ability to regenerate or mitigate exposure to potentially toxic agents. Previous reports show that HOCl can cause apoptosis and necrosis of tissue. HOCl produced by neutrophils during an inflammatory response has been shown to react with thiol groups and thioethers (Prütz, 1996), nucleotides and DNA (Prütz, 1996, 1998; Spencer et al., 2000), unsaturated fatty acids and cholesterol (Carr et al., 1996; Carr et al., 1997; Vissers et al., 1998; Winterbourn et al., 1992), and cell proteins (Armstrong & Buchanan, 1978; Hawkins & Davies, 1999; Hazell et al., 1999). In live tissue, HOCl damage is minimized by several mechanisms, including an irreversible reaction with glutathione, producing water (Forman et al., 2009). Zmuda et al. observed a reduction in cell viability after 24 h treatment with an HOCl-generating e-scaffold in an *ex vivo* biofilm model (Zmuda et al., 2020). Prolonged exposure to electrochemically-generated HOCl appears to negatively affect viability of porcine explant tissue. The observed toxicity could be mitigated by controlling HOCl delivery rate by operating the e-bandage at a lower working electrode potential, limiting the current delivered through the e-bandage, or operating the e-bandage with an intermittent polarization mode. Practically, there is a tradeoff between maximizing treatment efficacy by delivering HOCl into tissues at higher rates, and potential toxicity to the host tissue due to high HOCl concentrations. The e-bandage treatment could be tuned to operate at different modes based on clinical needs of specific infected wounds.

Overall, the developed HOCl-producing e-bandages inhibited *S. aureus* infections when explants were treated for 12 h immediately following inoculation, and reduced the viable *S. aureus* cells when 3-day-old mature biofilms were treated for 6, 12, and 24 h. In addition, transport of electrochemically-generated HOCl into biofilms and explants was documented in an *ex vivo* model. HOCl concentrations in the explant and biofilm varied between 30 and 80 μM and decreased with increasing distance from the e-bandage. Following treatment with polarized e-bandages, eukaryotic cell viability was reduced when compared to explants exposed to non-polarized e-bandages. Overall, the described e-bandage showed anti-biofilm activity in a porcine explant biofilm model.
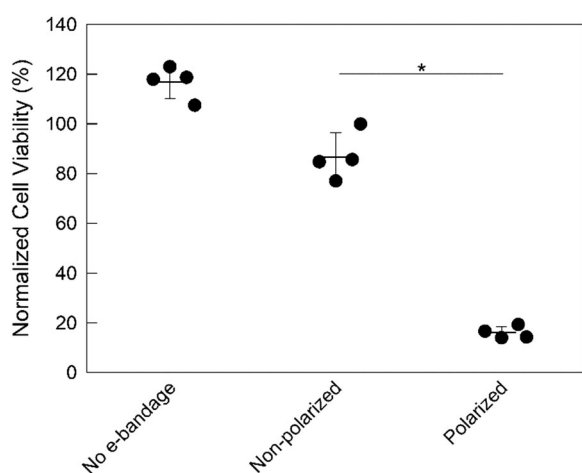

FIGURE 5 Effect of e-bandages on cell viability of uninfected explants. Normalized cell viability of explants with 12 h exposures to no e-bandage, nonpolarized e-bandages, or polarized e-bandages starting immediately after explant processing. Data points representing individual replicates are shown using circles. Horizontal lines and error bars represent averages and standard deviations. Statistical significance is indicated with a star (*n* = 4).
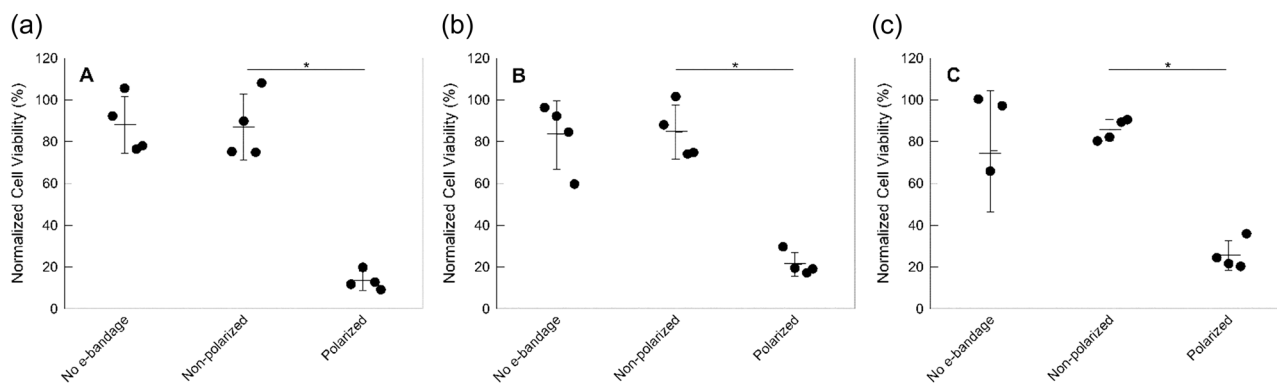

FIGURE 6 Effect of e-bandage treatment on cell viability of uninfected 3-day-old explants. Normalized cell viability of explants after (a) 6 h (h), (b) 12 h, and (c) 24 h treatment with no e-bandages, non-polarized e-bandages, or polarized e-bandages. Data points representing individual replicates are shown using circles. Horizontal lines and error bars represent averages and standard deviations. Statistical significance is indicated with a star (*n* = 4).

AUTHOR CONTRIBUTIONS

Gretchen Tibbits, Abdelrhman Mohamed, Suzanne Gelston, Laure Flurin, Yash S. Raval, Kerryl E. Greenwood-Quaintance, Robin Patel, and Haluk Beyenal developed the explant model. Gretchen Tibbits and Suzanne Gelston performed the explant processing and e-bandage experiments. Gretchen Tibbits and Abdelrhman Mohamed performed microelectrode measurements. Gretchen Tibbits wrote the initial draft. Haluk Beyenal and Robin Patel acquired the funding. Gretchen Tibbits, Abdelrhman Mohamed, Suzanne Gelston, Laure Flurin, Yash S. Raval, Kerryl E. Greenwood-Quaintance, Robin Patel and Haluk Beyenal participated in writing the manuscript.

ACKNOWLEDGMENTS

CONFLICTS OF INTEREST

HB holds a patent that describes electrochemical reduction or prevention of biofilm infections, which covers the operating principles of the electrochemical bandage.

DATA AVAILABILITY STATEMENT

The data that support the findings of this study are available from the corresponding author upon reasonable request.

ORCID

Gretchen Tibbits ⓘ http://orcid.org/0000-0002-4285-2258
Abdelrhman Mohamed ⓘ http://orcid.org/0000-0003-2132-0487
Suzanne Gelston ⓘ http://orcid.org/0000-0001-6853-8067
Laure Flurin ⓘ http://orcid.org/0000-0001-5687-1081
Yash S. Raval ⓘ http://orcid.org/0000-0003-1161-4000
Kerryl E. Greenwood-Quaintance ⓘ http://orcid.org/0000-0003-3760-4310
Robin Patel ⓘ http://orcid.org/0000-0001-6344-4141
Haluk Beyenal ⓘ http://orcid.org/0000-0003-3931-0244

REFERENCES

Alves, D. R., Booth, S. P., Scavone, P., Schellenberger, P., Salvage, J., Dedi, C., Thet, N.-T., Jenkins, A. T. A., Waters, R., Ng, K. W., Overall, A. D. J., Metcalfe, A. D., Nzakizwanayo, J., & Jones, B. V. (2018). Development of a high-throughput *ex-vivo* burn wound model using porcine skin, and its application to evaluate new approaches to control wound infection. *Frontiers in Cellular and Infection Microbiology*, 8(196). https://doi.org/10.3389/fcimb.2018.00196

Armstrong, D. A., & Buchanan, J. D. (1978). Reactions of O^{-2}, H_2O_2 and other oxidants with sulfhydryl enzymes. *Photochemistry and Photobiology*, 28(4–5), 743–754. https://doi.org/10.1111/j.1751-1097.1978.tb07011.x

Bien, J., Sokolova, O., & Bozko, P. (2011). Characterization of virulence factors of staphylococcus aureus: novel function of known virulence factors that are implicated in activation of airway epithelial proinflammatory response. *Journal of Pathogens*, 2011, 1–13. https://doi.org/10.4061/2011/601905

Carr, A. C., van den Berg, J. J. M., & Winterbourn, C. C. (1996). Chlorination of cholesterol in cell membranes by hypochlorous acid. *Archives of Biochemistry and Biophysics*, 332(1), 63–69. https://doi.org/10.1006/abbi.1996.0317

Carr, A. C., Vissers, M. C. M., Domigan, N. M., & Winterbourn, C. C. (1997). Modification of red cell membrane lipids by hypochlorous acid and haemolysis by preformed lipid chlorohydrins. *Redox Report*, 3(5–6), 263–271. https://doi.org/10.1080/13510002.1997.11747122

Chaney, S. B., Ganesh, K., Mathew-Steiner, S., Stromberg, P., Roy, S., Sen, C. K., & Wozniak, D. J. (2017). Histopathological comparisons of *Staphylococcus aureus* and *Pseudomonas aeruginosa* experimental infected porcine burn wounds. *Wound Repair and Regeneration*, 25(3), 541–549. https://doi.org/10.1111/wrr.12527

Davenport, E. K., Call, D. R., & Beyenal, H. (2014). Differential protection from tobramycin by extracellular polymeric substances from *Acinetobacter baumannii* and *Staphylococcus aureus* biofilms. *Antimicrobial Agents and Chemotherapy*, 58(8), 4755–4761. https://doi.org/10.1128/AAC.03071-14

Dowd, S. E., Sun, Y., Secor, P. R., Rhoads, D. D., Wolcott, B. M., James, G. A., & Wolcott, R. D. (2008). Survey of bacterial diversity in chronic wounds using pyrosequencing, DGGE, and full ribosome shotgun sequencing. *BMC Microbiology*, 8, 43. https://doi.org/10.1186/1471-2180-8-43

Driver, V. R., Fabbi, M., Lavery, L. A., & Gibbons, G. (2010). The costs of diabetic foot: the economic case for the limb salvage team. *Journal of Vascular Surgery*, 52(3 Suppl), 17S–22S. https://doi.org/10.1016/j.jvs.2010.06.003

Ehrensberger, M. T., Clark, C. M., Canty, M. K., & McDermott, E. P. (2020). Electrochemical methods to enhance osseointegrated prostheses. *Biomedical Engineering Letters*, 10(1), 17–41. https://doi.org/10.1007/s13534-019-00134-8

Flurin, L., Raval, Y. S., Mohamed, A., Greenwood-Quaintance, K. E., Cano, E. J., Beyenal, H., & Patel, R. (2021). An integrated HOCl-producing e-scaffold is active against monomicrobial and polymicrobial biofilms. *Antimicrobial Agents and Chemotherapy*, 65(3). https://doi.org/10.1128/aac.02007-20

Forman, H. J., Zhang, H., & Rinna, A. (2009). Glutathione: Overview of its protective roles, measurement, and biosynthesis. *Molecular Aspects of Medicine*, 30(1–2), 1–12. https://doi.org/10.1016/j.mam.2008.08.006

Gupta, P., Sarkar, S., Das, B., Bhattacharjee, S., & Tribedi, P. (2016). Biofilm, pathogenesis and prevention–a journey to break the wall: A review. *Archives of Microbiology*, 198(1), 1–15. https://doi.org/10.1007/s00203-015-1148-6

Hawkins, C. L., & Davies, M. J. (1999). Hypochlorite-induced oxidation of proteins in plasma: formation of chloramines and nitrogen-centred radicals and their role in protein fragmentation. *Biochemical Journal*, 340(Pt 2), 539–548.

Hawkins, C. L. (2019). Hypochlorous acid-mediated modification of proteins and its consequences. *Essays in Biochemistry*, 64(1), 75–86. https://doi.org/10.1042/ebc20190045

Hazell, L. J., Davies, M. J., & Stocker, R. (1999). Secondary radicals derived from chloramines of apolipoprotein B-100 contribute to

HOCl-induced lipid peroxidation of low-density lipoproteins. *Biochemical Journal*, *339*(Pt 3), 489–495.

Heald, R., Salyer, S., Ham, K., Wilgus, T. A., Subramaniam, V. V., & Prakash, S. (2022). Electroceutical treatment of infected chronic wounds in a dog and a cat. *Veterinary Surgery*, *51*(3), 520–527. https://doi.org/10.1111/vsu.13758

Hiramatsu, K., Hanaki, H., Ino, T., Yabuta, K., Oguri, T., & Tenover, F. C. (1997). Methicillin-resistant *Staphylococcus aureus* clinical strain with reduced vancomycin susceptibility. *Journal of Antimicrobial Chemotherapy*, *40*(1), 135–136. https://doi.org/10.1093/jac/40.1.135

Høiby, N., Ciofu, O., Johansen, H. K., Song, Z., Moser, C., Jensen, P.Ø., Molin, S., Givskov, M., Tolker-Nielsen, T., & Bjarnsholt, T. (2011). The clinical impact of bacterial biofilms. *International Journal of Oral Science*, *3*(2), 55–65. https://doi.org/10.4248/ijos11026

Huiszoon, R. C., Han, J., Chu, S., Stine, J. M., Beardslee, L. A., & Ghodssi, R. (2021). Integrated system for bacterial detection and biofilm treatment on indwelling urinary catheters. *IEEE Transactions on Biomedical Engineering*, *68*(11), 3241–3249. https://doi.org/10.1109/TBME.2021.3066995

Jensen, L. K., Johansen, A. S. B., & Jensen, H. E. (2017). Porcine models of biofilm infections with focus on pathomorphology. *Frontiers in Microbiology*, *8*(1961). https://doi.org/10.3389/fmicb.2017.01961

Kiamco, M. M., Zmuda, H. M., Mohamed, A., Call, D. R., Raval, Y. S., Patel, R., & Beyenal, H. (2019). Hypochlorous-acid-generating electrochemical scaffold for treatment of wound biofilms. *Scientific Reports*, *9*(1), 2683. https://doi.org/10.1038/s41598-019-38968-y

Koch, G., Yepes, A., Förstner, K. U., Wermser, C., Stengel, S. T., Modamio, J., Ohlsen, K., Foster, K. R., & Lopez, D. (2014). Evolution of resistance to a last-resort antibiotic in *Staphylococcus aureus* via bacterial competition. *Cell*, *158*(5), 1060–1071. https://doi.org/10.1016/j.cell.2014.06.046

Lewandowski, Z., & Beyenal, H. (2013). *Fundamentals of biofilm research* (2nd ed.). CRC Press.

Lochab, V., Jones, T. H., Dusane, D. H., Peters, C. W., Stoodley, P., Wozniak, D. J., Subramaniam, V. V., & Prakash, S. (2020). Ultrastructure imaging of Pseudomonas aeruginosa lawn biofilms and eradication of the tobramycin-resistant variants under in vitro electroceutical treatment. *Scientific Reports*, *10*, 9879. https://doi.org/10.1038/s41598-020-66823-y

Lone, A. G., Atci, E., Renslow, R., Beyenal, H., Noh, S., Fransson, B., Abu-Lail, N., Park, J.-J., Gang, D. R., & Call, D. R. (2015). *Staphylococcus aureus* induces hypoxia and cellular damage in porcine dermal explants. *Infection and Immunity*, *83*(6), 2531–2541. https://doi.org/10.1128/IAI.03075-14

McMahon, R., Salamone, A. B., Poleon, S., Bionda, N., & Salamone, J. (2020). Efficacy of wound cleansers on wound-specific organisms using in vitro and exvivo biofilm models. *Wound Management & Prevention*, *66*(11), 31–42.

Metcalf, D. G., & Bowler, P. G. (2013). Biofilm delays wound healing: A review of the evidence. *Burns & Trauma*, *1*(1), 5–12. https://doi.org/10.4103/2321-3868.113329

Mohamed, A., Anoy, M. M. I., Tibbits, G., Raval, Y. S., Flurin, L., Greenwood-Quaintance, K. E., Patel, R., & Beyenal, H. (2021). Hydrogen peroxide-producing electrochemical bandage controlled by a wearable potentiostat for treatment of wound infections. *Biotechnology and Bioengineering*, *118*(7), 2815–2821. https://doi.org/10.1002/bit.27794

Nadell, C. D., Xavier, J. B., & Foster, K. R. (2009). The sociobiology of biofilms. *FEMS Microbiology Reviews*, *33*(1), 206–224. https://doi.org/10.1111/j.1574-6976.2008.00150.x

Nakatsuji, T., Chen, T. H., Two, A. M., Chun, K. A., Narala, S., Geha, R. S., Hata, T. R., & Gallo, R. L. (2016). *Staphylococcus aureus* exploits epidermal barrier defects in atopic dermatitis to trigger cytokine expression. *Journal of Investigative Dermatology*, *136*(11), 2192–2200. https://doi.org/10.1016/j.jid.2016.05.127

Phillips, P. L., Yang, Q., Davis, S., Sampson, E. M., Azeke, J. I., Hamad, A., & Schultz, G. S. (2015). Antimicrobial dressing efficacy against mature *Pseudomonas aeruginosa* biofilm on porcine skin explants. *International Wound Journal*, *12*(4), 469–483. https://doi.org/10.1111/iwj.12142

Prütz, W. A. (1996). Hypochlorous acid interactions with thiols, nucleotides, DNA, and other biological substrates. *Archives of Biochemistry and Biophysics*, *332*(1), 110–120. https://doi.org/10.1006/abbi.1996.0322

Prütz, W. A. (1998). Interactions of hypochlorous acid with pyrimidine nucleotides, and secondary reactions of chlorinated pyrimidines with GSH, NADH, and other substrates. *Archives of Biochemistry and Biophysics*, *349*(1), 183–191. https://doi.org/10.1006/abbi.1997.0440

Raval, Y. S., Flurin, L., Mohamed, A., Greenwood-Quaintance, K. E., Beyenal, H., & Patel, R. (2021). *In vitro* antibacterial activity of hydrogen peroxide and hypochlorous acid, including that generated by electrochemical scaffolds. *Antimicrobial Agents and Chemotherapy*, *65*(5), e01966–01920. https://doi.org/10.1128/AAC.01966-20

Rhoads, D. D., Cox, S. B., Rees, E. J., Sun, Y., & Wolcott, R. D. (2012). Clinical identification of bacteria in human chronic wound infections: Culturing vs. 16S ribosomal DNA sequencing. *BMC Infectious Diseases*, *12*(1), 321. https://doi.org/10.1186/1471-2334-12-321

Roberts, A. E. L., Powell, L. C., Pritchard, M. F., Thomas, D. W., & Jenkins, R. E. (2019). Anti-pseudomonad activity of Manuka honey and antibiotics in a specialized *ex vivo* model simulating cystic fibrosis lung infection. *Frontiers in Microbiology*, *10*, 869. https://doi.org/10.3389/fmicb.2019.00869

Roche, E. D., Woodmansey, E. J., Yang, Q., Gibson, D. J., Zhang, H., & Schultz, G. S. (2019). Cadexomer iodine effectively reduces bacterial biofilm in porcine wounds *ex vivo* and *in vivo*. *International wound journal*, *16*(3), 674–683. https://doi.org/10.1111/iwj.13080

Rumble, J. R. (1978). CRC Handbook of Chemistry and Physics.

Sayedyahossein, S., Xu, S. X., Rudkouskaya, A., McGavin, M. J., McCormick, J. K., & Dagnino, L. (2015). *Staphylococcus aureus* keratinocyte invasion is mediated by integrin-linked kinase and Rac1. *The FASEB Journal*, *29*(2), 711–723. https://doi.org/10.1096/fj.14-262774

Sen, C. K. (2019). Human wounds and its burden: An updated compendium of estimates. *Advances in Wound Care*, *8*(2), 39–48. https://doi.org/10.1089/wound.2019.0946

Sen, C. K., Gordillo, G. M., Roy, S., Kirsner, R., Lambert, L., Hunt, T. K., Gottrup, F., Gurtner, G. C., & Longaker, M. T. (2009). Human skin wounds: A major and snowballing threat to public health and the economy. *Wound Repair and Regeneration*, *17*(6), 763–771. https://doi.org/10.1111/j.1524-475X.2009.00543.x

Spencer, J. P., Whiteman, M., Jenner, A., & Halliwell, B. (2000). Nitrite-induced deamination and hypochlorite-induced oxidation of DNA in intact human respiratory tract epithelial cells. *Free Radical Biology and Medicine*, *28*(7), 1039–1050. https://doi.org/10.1016/s0891-5849(00)00190-8

Sullivan, T. P., Eaglstein, W. H., Davis, S. C., & Mertz, P. (2001). The pig as a model for human wound healing. *Wound Repair and Regeneration*, *9*(2), 66–76. https://doi.org/10.1046/j.1524-475x.2001.00066.x

Sultana, S. T., Babauta, J. T., & Beyenal, H. (2015). Electrochemical biofilm control: A review. *Biofouling*, *31*(9–10), 745–758. https://doi.org/10.1080/08927014.2015.1105222

Tibbits, G., Mohamed, A., Gelston, S., Flurin, L., Raval, Y. S., Greenwood-Quaintance, K., Patel, R., & Beyenal, H. (2022). Efficacy and toxicity of hydrogen peroxide producing electrochemical bandages in a porcine explant biofilm model. *Journal of Applied Microbiology*, n/a(n/a). https://doi.org/10.1111/jam.15812

Ulfig, A., & Leichert, L. I. (2021). The effects of neutrophil-generated hypochlorous acid and other hypohalous acids on host and pathogens. *Cellular and Molecular Life Sciences*, *78*(2), 385–414. https://doi.org/10.1007/s00018-020-03591-y

Uruén, C., Chopo-Escuin, G., Tommassen, J., Mainar-Jaime, R. C., & Arenas, J. (2021). Biofilms as promoters of bacterial antibiotic resistance and tolerance. *Antibiotics (USSR)*, *10*(1), 3. https://doi.org/10.3390/antibiotics10010003

Vissers, C. M. M., Carr, C. A., & Chapman, L. P. A. (1998). Comparison of human red cell lysis by hypochlorous and hypobromous acids: Insights into the mechanism of lysis. *Biochemical Journal*, *330*(Pt 1), 131–138. https://doi.org/10.1042/bj3300131

Walsh, C., & Wencewicz, T. A. (2016). *Antibiotics: challenges, mechanisms, opportunities*. ASM Press.

Wang, H., Agrawal, A., Wang, Y., Crawford, D. W., Siler, Z. D., Peterson, M. L., Woofter, R. T., Labib, M., Shin, H. Y., Baumann, A. P., & Phillips, K. S. (2021). An ex vivo model of medical device-mediated bacterial skin translocation. *Scientific Reports*, *11*, (1), 5746. https://doi.org/10.1038/s41598-021-84826-1

Wang, Y., Tan, X., Xi, C., & Phillips, K. S. (2018). Removal of *Staphylococcus aureus* from skin using a combination antibiofilm approach. *NPJ Biofilms and Microbiomes*, *4*(1), 16. https://doi.org/10.1038/s41522-018-0060-7

Winter, J., Ilbert, M., Graf, P. C. F., Özcelik, D., & Jakob, U. (2008). Bleach activates a redox-regulated chaperone by oxidative protein unfolding. *Cell*, *135*(4), 691–701. https://doi.org/10.1016/j.cell.2008.09.024

Winterbourn, C. C., van den Berg, J. J. M., Roitman, E., & Kuypers, F. A. (1992). Chlorohydrin formation from unsaturated fatty acids reacted with hypochlorous acid. *Archives of Biochemistry and Biophysics*, *296*(2), 547–555. https://doi.org/10.1016/0003-9861(92)90609-z

Yang, Q., Larose, C., Della Porta, A. C., Schultz, G. S., & Gibson, D. J. (2017). A surfactant-based wound dressing can reduce bacterial biofilms in a porcine skin explant model. *International Wound Journal*, *14*(2), 408–413. https://doi.org/10.1111/iwj.12619

Yang, Q., Phillips, P. L., Sampson, E. M., Progulske-Fox, A., Jin, S., Antonelli, P., & Schultz, G. S. (2013). Development of a novel ex vivo porcine skin explant model for the assessment of mature bacterial biofilms. *Wound Repair and Regeneration*, *21*(5), 704–714. https://doi.org/10.1111/wrr.12074

Zmuda, H. M., Mohamed, A., Raval, Y. S., Call, D. R., Schuetz, A. N., Patel, R., & Beyenal, H. (2020). Hypochlorous acid-generating electrochemical scaffold eliminates *Candida albicans* biofilms. *Journal of Applied Microbiology*, *129*(4), 776–786. https://doi.org/10.1111/jam.14656

SUPPORTING INFORMATION

Additional supporting information can be found online in the Supporting Information section at the end of this article.

How to cite this article: Tibbits, G., Mohamed, A., Gelston, S., Flurin, L., Raval, Y. S., Greenwood-Quaintance, K. E., Patel, R., & Beyenal, H. (2023). Activity of a hypochlorous acid-producing electrochemical bandage as assessed with a porcine explant biofilm model. *Biotechnology and Bioengineering*, 120, 250–259. https://doi.org/10.1002/bit.28248